HHS Public Access

Author manuscript

Immunity. Author manuscript; available in PMC 2018 November 21.

Published in final edited form as:

Immunity. 2017 November 21; 47(5): 862–874.e3. doi:10.1016/j.immuni.2017.10.020.

MIGRATING MYELOID CELLS SENSE TEMPORAL DYNAMICS OF CHEMOATTRACTANT CONCENTRATIONS

Caren E. Petrie Aronin[1,#], **Yun Zhao**[1,#], **Justine S. Yoon**[2], **Nicole Y. Morgan**[2], **Thorsten Prüstel**[3], **Ronald N. Germain**[1,*], and **Martin Meier-Schellersheim**[3,*]

[1]Laboratory of Systems Biology (LSB), Lymphocyte Biology Section (LBS), National Institute of Allergy and Infectious Disease, National Institutes of Health, Bethesda, Maryland 20892, USA

[2]Biomedical Engineering and Physical Sciences Resource (BEPS), Microfabrication and Microfluidics Unit (MMU), National Institute of Biomedical Imaging and Bioengineering, National Institutes of Health, Bethesda, Maryland 20892, USA

[3]Laboratory of Systems Biology (LSB), Computational Biology Unit (CBU), National Institute of Allergy and Infectious Disease, National Institutes of Health, Bethesda, Maryland 20892, USA

Summary

Chemoattractant-mediated recruitment of hematopoietic cells to sites of pathogen growth or tissue damage is critical to host defense and organ homeostasis. Chemotaxis is typically considered to rely on spatial sensing, with cells following concentration gradients as long as these are present. Utilizing a microfluidic approach, we found that stable gradients of intermediate chemokines (CCL19 and CXCL12) failed to promote persistent directional migration of dendritic cells or neutrophils. Instead, rising chemokine concentrations were needed, implying that temporal sensing mechanisms controlled prolonged responses to these ligands. This behavior was found to depend on G-coupled receptor kinase-mediated negative regulation of receptor signaling and contrasted with responses to an end agonist chemoattractant (C5a), for which a stable gradient led to persistent migration. These findings identify temporal sensing as a key requirement for long-range myeloid cell migration to intermediate chemokines and provide insights into the mechanisms controlling immune cell motility in complex tissue environments.

Introduction

The ability of the immune system to develop organized lymphoid tissues, respond to tissue damage, and mount effective responses towards pathogenic challenges critically depends on the spatio-temporal coordination of hematopoietic cell migration and positioning. Chemokines play an essential role in these developmental (van de Pavert and Mebius, 2010)

*Co-corresponding authors: rgermain@niaid.nih.gov and mms@niaid.nih.gov.
#Equal contributions
Lead Contact: Martin Meier-Schellersheim (mms@niaid.nih.gov)

and host defense processes (Rot and von Andrian, 2004), where they control cell migratory behavior, steady-state positioning (Link et al., 2007), and the efficiency of interactions between rare cell subpopulations (Castellino et al., 2006).

Eukaryotic chemotaxis is a remarkably sensitive process with chemoattractant concentration differences of few percent across the cell diameter being sufficient to induce cell polarization and promote migration along the sensed gradient. The molecular mechanisms regulating such cellular responses to even shallow chemoattractant fields have not been fully elucidated but the overwhelming majority of hypotheses suggests that eukaryotic cells respond to spatial concentration differences (Parent and Devreotes, 1999), in contrast to bacteria that analyze temporal changes to bias their tumbling motion towards nutrient sources (Macnab and Koshland, 1972). Early studies on eukaryotic chemotaxis considered both spatial and temporal characteristics of the chemoattractant signal as potentially important in cell guidance (Lauffenburger et al., 1987; Lauffenburger et al., 1988; Vicker, 1989; Vicker et al., 1986). A major subject of contention in trying to assess the relative importance of these two modes of migratory control has been uncertainty over what local concentration differences cells experience in various experimental systems and more so, *in vivo*, with particular concern about whether presumed stable gradients were indeed stable or whether they were subject to temporal variations. The latter could be either due to differences between the initial and later plateau phases of gradient development or to movement of the cells within spatially heterogeneous chemoattractant fields that would result in temporally changing local concentration environments. In either case, the existence of such variations would have a major impact on how the data are interpreted.

Despite such considerations and available evidence that fluctuations in chemoattractant concentrations can indeed modulate cellular migration behavior (Ebrahimzadeh et al., 2000) a clear consensus that hematopoietic cells use spatial sensing to guide their polarization and long-distance directional movement has emerged in the field. Several models have in turn been developed to explain how cells reliably translate a stable, often very shallow, gradient of an extracellular stimulus into an intracellular polarized response that guides sustained directional migration (Arrieumerlou and Meyer, 2005; Charest and Firtel, 2006; Levine et al., 2006; Ma et al., 2004; Meier-Schellersheim et al., 2006; Meinhardt, 1999; Postma and Van Haastert, 2001). The most widely accepted model postulates that the difference in the degree of receptor ligation between the sides of the cell experiencing the highest and the lowest chemoattractant concentrations drives polarized actin dynamics, which then promotes persistent cell movement in the direction of the upward slope of the gradient (Parent and Devreotes, 1999).

However, in the context of immune cell recruitment within complex environments, there is evidence that hierarchies of chemotactic signals direct cellular migration to and within target tissues, indicating that the control of chemotactic responses clearly goes beyond the action of single spatial cues (Campbell et al., 1997). Receptor desensitization plays an essential role in such multi-step navigation during which cells respond to newly emerging or initially distant signals (Foxman et al., 1997; Lin and Butcher, 2008; Wu and Lin, 2011) but the mechanism by which certain chemoattractants (‘end point agonists’) can provide dominant guidance whereas others (‘intermediate chemokines’) function as less persistent directional

cues has not yet been clearly identified. A related issue is the extent to which soluble vs. matrix-bound stimuli direct cell movement. While gradients of immobilized chemokines have been shown to play a role in directional cell guidance *in vivo* (Sarris et al., 2012; Weber et al., 2013), not all chemoattractants act in this manner. CCL19, an agonist closely related to CCL21, lacks the C-terminus needed to bind matrix proteins (Nagira et al., 1997; Tanabe et al., 1997), and it is unknown whether lipids such as S1P and LPA or protein fragments such as C5a and fMLP can bind to extracellular matrix proteins or if they form only soluble gradients.

Given these many uncertainties about how migration and positioning are regulated, especially in complex 3D environments, we adopted and modified a microfabricated 3D migration chamber system first described by Haessler et al. (Haessler et al., 2009) and used this device to obtain quantitative data about how gradients of soluble chemoattractants control the directed migration of dendritic cells and neutrophils, cell populations that play key roles during the onset and for the regulation of local immune responses. In contrast to what would be expected based on guidance control involving only spatial gradient sensing, these studies surprisingly revealed that neither cell type showed persistent directional migration in stable gradients of CCL19 or CXCL12 across a wide range of steepness. Further analysis revealed that this behavior reflected the operation of a potent negative feedback mechanism involving G-coupled receptor kinases (GRKs) that led to rapid cellular adaptation to the existing gradient. Continued migration required a temporally rising chemoattractant stimulus, with the cells moving along a preexisting direction of polarization. This requirement for temporal sensing was observed for chemoattractants (CCL19 and CXCL12) that are classified as ‘intermediate chemokines’ whereas C5a, a member of another class of compounds termed ‘end agonist’ chemoattractants, induced persistent movement when provided as a stable gradient. Thus, our findings reveal a striking dependence of the mode of immune cell chemotactic behavior on the class of ligand, and require a modification of the predominant, purely spatial model for control of long-range cell guidance in complex tissue environments with multiple chemoattractant sources whose strengths often vary over time.

Results

A microfluidic platform establishes a defined soluble chemokine gradient in a 3D collagen network

To generate defined 3D soluble gradients of chemokine across a collagen fiber scaffold, we employed a microfluidic platform first described by Haessler et al. (Haessler et al., 2009) in which chemokine source and sink channels are separated from the cell-matrix compartment by an agarose barrier (Figure S1A–E). This porous barrier prevents convective fluid flow but allows passive chemokine diffusion and gradient development across the cell channel, thus removing the effects of shear flow from our analysis of cellular responses towards chemokine gradients. Utilizing programmable syringe pumps operating in parallel to control flow profiles in both source and sink channels, steady-state and rising concentrations of diffusing chemokine can be established. This setup, combined with time-lapse microscopy

permitted image capture of cell shape changes (Movie S1) and migratory trajectories in response to definable chemokine gradient profiles.

Dendritic cells migrate only transiently during the formation of a CCL19 gradient

We first examined the CCR7-dependent migration of fluorescent reporter (CD11c-EYFP) bone marrow-derived mature dendritic cells (BMDCs) in response to the chemokine CCL19 that binds CCR7 with a Kd of about 1.5 nM (Comerford et al., 2006). Unlike many chemokines, CCL19 lacks the positively charged C-terminus that binds these mediators to a variety of proteoglycans and matrix proteins (Yoshida et al., 1998). This permitted the formation of well-defined soluble CCL19 gradients without the added complexity of association with extracellular components in our experimental system. Labeled Alexa-Fluor 594-CCL19 was utilized in initial gradient characterization studies to ensure that bulk chemokine gradients were not significantly disturbed by local cellular uptake and migration (Figure S2A–B). Alexa-Fluor 594-CCL19 diffuses similarly to 10kDa FITC-dextran (Figure S2C–D) and this latter molecule was used for all subsequent gradient characterization studies (Figure S2E–M).

BMDCs exposed to CCL19 revealed the expected directed migration during early times after initial contact with the developing gradient, but surprisingly, lost gradient-oriented directional migration persistence once a stable gradient state was reached (Movie S2). Our 3D system relies on passive chemokine diffusion from the source channel across the porous agarose barrier into the subsequent cell-matrix channel. Therefore, during ‘de novo’ gradient formation cells do not immediately experience steady-state concentrations but rather continuously rising chemoattractant concentrations for approximately 30 minutes (Figure 1A, B). Note, however, that the slope of the gradient becomes stable very soon while the *absolute* concentration rises.

To determine whether there was a relationship between the rising concentrations in a forming gradient and the movement of the DC in response to CCL19, we conducted a careful kinetic study. This time-resolved analysis of BMDC migration revealed that significant displacement towards the CCL19 source occurred almost exclusively during the first 30 minutes during which CCL19 concentrations were still rising (Figure 1C, D). Additionally, cellular forward protrusions became significantly less aligned toward the source channel once steady state gradients were fully established (40min – 60min (Figure 1E)). Establishing a gradient in the agarose device prior to the introduction of cells (referred to as ‘pre-set’ gradient in Figure 1 and in Figures 2, 4 and S4 as ‘stable’) reduced the time for stable gradient formation to 10 minutes and led to a corresponding decrease in the duration of BMDC directional migration persistence (Figure 1F, Movie S3). This phenomenon of transient directional movement limited to the gradient formation stage was seen across a wide-range of absolute CCL19 concentrations and relative gradient steepness. While there was a slight increase in directed cell migration in the secondary (stable gradient) phase for very steep gradients this increase did not reach statistical significance (Figure S3A, and Figure S2N).

A critical issue was whether the environment in the chamber caused a loss of cell homeostasis, viability, or signaling capacity, accounting for the failure of the BMDCs to

show persistent migration for longer than 30 minutes. Several controls were performed to test for such effects. Cells incubated in the chamber for 1 hour and then provided a rising source concentration showed robust directed migration similar to that of cells provided the same stimulus immediately after seeding (Figure S3B–E). These findings argue against a loss of viability or motile capacity among the BMDC as the basis for the short duration of continued migration in the preceding experiments. Likewise, cells that had stopped migrating after being held in a fully-developed stable gradient for 25 minutes subsequently showed a significant increase in cell velocity and migratory persistence when exposed to a further increase in source concentration (Figure S3F-H, Movie S4), indicating that such cells are still capable of responding to rising inputs and have not become unresponsive, saturated in receptor occupancy, or unhealthy. Finally, neither gradient steepness nor chemokine concentration *per se* dictated the failure of cells to migrate persistently in stable gradients. (Figure S3A and Figure S2N). Given this evidence against an artifactual explanation for the failure of BMDC to show persistent migration in a stable CCL19 gradient, we considered the alternative: that cellular sensing of temporally rising concentrations of this chemokine was required for long-range persistent BMDC chemotaxis.

BMDC show persistent directional migration in a rising CCL19 gradient

To investigate this possibility more thoroughly, we examined cellular responses under controllable conditions in which we could provide either stable or continuously rising source chemokine concentrations. Indeed, rather than ceasing directional migration after 30–40 minutes, BMDCs exposed to continuously rising source chemokine (Figure 2A) responded with robust migration towards the CCL19 source that persisted during the entire 1.5 hours of image capture (Figure 2B, and Movie S5). Gradient-aligned migratory persistence, the ratio of displacement along the gradient to the total path length, was significantly greater with continuously rising source concentrations than with stable inputs (Figure 2C). Individual cell velocities in continuously rising groups remained at 1.8 μm/min for the duration of the experiment vs. a much lower 0.3 μm/min for cells in stable gradients (Figure 2D). Additionally, we observed a substantial shift to higher population speeds of cells exposed to continuously rising inputs as compared to those in stable gradients (Figure 2E) and the percent of migrating cells within a population was higher (82% compared with 57%), for cells exposed to continuously rising source concentrations as compared to those in stable gradients. Importantly, directed migration persisted well after the gradient steepness reached a steady state equivalent to that of the stable gradients (Figure S2K, L). This further indicated that the persistent migration in rising chemokine concentrations was not due to distinct spatial characteristics such as gradient slope but rather depended on the increasing absolute concentration of chemoattractant.

In further support of a temporal sensing mechanism, chemotactic dynamics appeared well tuned with source chemokine dynamics. Dendritic cell velocities were correlated with the rates of source concentration rise (Figure S3I, J) and directed chemotaxis under continuously rising conditions was consistent with receptor occupancy and saturation principles. Migratory persistence along the gradient, forward protrusion alignment, and speed distributions were greatest at 5–10 nM of CCL19 (Figure S3K–O), suggesting that BMDC migratory response increased as the CCL19 concentration reached a few-fold of the ligand-

receptor K_D but became less pronounced at higher concentrations. Having established the influence of the temporal characteristics of these chemokine gradients on cell migration, we shifted our focus toward identifying which cellular signaling components or mechanisms might account for the observed behavior.

GRK-mediated receptor desensitization interferes with persistent migration

The requirement for continuously rising source chemokine to drive persistent directed migration suggested that receptor desensitization might contribute to this behavior. We speculated that as a cell moves up a stable gradient, desensitization or adaptation could reduce the signal available to the cell to such a low level that it becomes insufficient to sustain continuing migration. This limitation could, however, be overcome by exposure to a temporal increase in the absolute amount of available ligand. The soluble chemokine CCL19, along with its receptor, CCR7, are internalized via a clathrin-mediated process involving β-arrestin-2, GRK6 (G protein-coupled receptor kinase 6) (receptor phosphorylation), and GRK3 (receptor desensitization) (Byers et al., 2008; Kohout et al., 2004; Ren et al., 2005; Wisler et al., 2014; Zidar et al., 2009). We therefore tested whether cells from animals deficient in any of these regulatory molecules showed spatial rather than temporal sensing requirements for persistent migration to CCL19, as such a model would predict. With regard to the comparison between exposure to stable vs. to rising inputs, mature dendritic cells isolated from bone marrow of β-arrestin-2-, β-arrestin-1-, and GRK6-deficient animals showed very similar behavior as wild-type cells (Figure S4A–D). Consistent with other reports that suggest that removal of such negative regulatory components enhance chemotaxis (Balabanian et al., 2008; Kavelaars et al., 2003), β-arrestin-1-deficient cells showed higher velocities relative to WT cells in continuously rising source conditions. Moreover, all three mutant populations showed stronger persistence in rising gradients of CCL19, albeit at a lower absolute level than wild-type cells did in response to CXCL12. GRK6, in particular, appears to play complex roles, as indicated by the fact that it recently was found to be important for chemotaxis along surface-bound gradients while being dispensable for soluble ones (Schwarz et al., 2017).

In clear contrast to the properties of wild-type, β-arrestin-2 deficient, β-arrestin-1 deficient, or GRK6 deficient cells, BMDCs isolated from *Grk3*$^{-/-}$ mice showed robust migration in both stable and continuously rising source conditions, as measured by migratory persistence, cell speeds, and forward protrusion alignments (Figure 3A–D). To minimize any possible differences in the gradient conditions experienced by WT and mutant cells during these analyses, we directly compared the spatiotemporal chemotactic response of BMDCs isolated from CD11c-EYFP and DsRed *Grk3*$^{-/-}$ mice to rising then stable and continuously rising CCL19 gradients using mixed populations examined simultaneously in the same migration chamber (Movie S6–S7). To avoid selection bias in identifying cells for tracking, the videos were re-named and re-colored by a third party before collection of migration data so that the identities of the cells being tracked and the gradient conditions were not known until the color code was revealed after the tracking data had been processed. The data from these co-migration experiments are consistent with receptor desensitization promoting dependence on temporal sensing for persistent directional migration of WT BMDCs in response to CCL19. Removing the negative regulator GRK3 presumably limits desensitization, thus permitting

prolonged directed migration in stable gradients. For CCL19 interacting with CCR7, receptor desensitization is promoted by GRK3 whereas β-arrestin mediated signaling is promoted by GRK6 (Byers et al., 2008; Ren et al., 2005; Wisler et al., 2014). These biochemical observations are consistent with our migration data, suggesting GRK3-mediated control for CCL19-triggered CCR7 desensitization. However, it remained to be seen whether similar observations could be made with other chemokine pathways or cell types.

Chemoattractant class dictates operation of spatial vs. temporal sensing modalities

Neutrophils have been a major focus for studies of migration control among immune cells. Therefore, in an effort to determine whether the observed role of temporal chemokine sensing in directed movement of dendritic cells applies more widely to other immune cells and chemokines, comparisons between rising and stable inputs were undertaken utilizing freshly isolated neutrophils from bone marrow and the chemoattractant C5a that binds to its receptor on leukocytes with a Kd of about 1nM (Chenoweth and Goodman, 1983). In contrast to the data with CCL19 and BMDCs, neutrophils migrated to C5a equally well under both continuously rising and stable conditions, showing similar directional persistence (Figure 4A, Movie S8, S9) and speed distributions (Figure S4G) in the two situations.

Previous work on neutrophil chemotaxis led to the development of a nomenclature that categorized chemoattractants into two classes, ‘intermediate’ and ‘end agonist’. The two classes of ligands were proposed to play distinct roles in the guidance of immune cells at different steps in their migration from blood to an infected or wounded site (Foxman et al., 1997). Prior studies suggested a hierarchical arrangement of desensitization mechanisms for the receptors for the different ligand types, in which intermediate chemokines display homologous desensitization, whereas end-point chemoattractants such as C5a demonstrate heterologous desensitization, thought to occur independently of GRKs (Milcent et al., 1999). This suggested the possibility that there might be distinct rules for control of cell movement depending on ligand class. If so, then the qualitative differences we observed using CCL19 (an intermediate chemokine using the neutrophil conventions) and C5a (an end agonist by these definitions) might not be due to differences in BMDC vs. neutrophil chemosensing mechanisms but rather to the specific ligand employed. We therefore conducted additional experiments using BMDCs and neutrophils with representatives of the two different chemoattractant classes. With another intermediate chemokine, CXCL12, both mature DCs and fresh neutrophils showed differences in chemotaxis between stable and continuously rising conditions exhibiting behavior similar to that seen using CCL19 and BMDCs (Figure 4B, C, Figure S4H, I). In contrast, immature BMDCs that express the C5a receptor showed migration behavior similar to that of neutrophils in response to the end agonist C5a, with no significant differences in migration between stable and rising inputs (Figure 4D, Figure S4J). These findings strongly suggest that it is the nature of the chemoattractant receptor-ligand pair, and not the cell type, that dictates the requirement for temporal sensing in promoting sustained directional responses.

Spatial and temporal sensing play sequential roles for persistent directional migration

Given that BMDC and neutrophils show directional movement up the slope of a gradient even when temporal sensing is necessary for persistent migration to intermediate

chemokines, we suspected that orientation of a cell along the gradient arises from a transient phase of spatial sensing when the cell first experiences the chemoattractant. This initial polarization would be followed by sensory adaptation and a requirement for a rising chemoattractant concentration to promote continued migration in this pre-established direction. To test this hypothesis, we pre-soaked the agarose chamber device with defined CCL19 concentrations (pre-soak) (Figure 5A). In contrast to the developing gradient under our standard experimental setup (immediate), pre-soaking allowed exposure of BMDCs to a spatially homogeneous stimulus with stochastic distributions of cell polarity directions (Figure 5C, early tracks distinguished by color scale bar). Subsequent introduction of a spatial gradient with continuously rising source concentration evoked persistent migration in the direction of polarization acquired at the time of gradient development. BMDCs did not re-align to move along the new spatial gradient (Figure 5B, C, Movie S10), confirming that the pivotal element at later time points was the temporally rising concentration and that spatial sensing, which would be expected to result in re-orientation of the cells along the gradient slope, did not occur. Additional presoaking experiments revealed that neutrophils showed stochastic polarization in both homogeneous CXCL12 and C5a fields in a similar manner to BMDCs prior to the introduction of continuously rising chemokine input. Confirming our findings that the mechanisms by which intermediate chemokines guide sustained chemotactic motion differ from those used by end agonist chemokines, subsequent introduction of a rising spatial CXCL12 gradient caused neutrophils to persist along initial trajectories (Figure 5D, E) whereas the imposition of a spatial C5a gradient caused neutrophils to re-orient and migrate up the gradient (Figure 5F, G, Movie S11). Collectively, these data imply that while cellular sensing of temporally rising concentrations is required for persistent cell chemotaxis in 3D soluble intermediate chemokine gradients, early spatial cues (front-rear concentration differences) may control the initial direction of cell polarization in such situations (Table 1) and explain the directional nature of migration even when temporal sensing is controlling long-term cell movement.

A closer examination of the early spatial cues in the pre-soaking experiments revealed that leukocytes, on average, had negligible net displacement (less than two cell diameters) in homogeneous chemokine fields after 10 minutes of imaging (Figure S5A–F), exhibiting characteristic stochastic turning behavior in this condition of uniform chemoattractant. The homogeneous chemokine field was generated using chemokines at concentration ranges within their respective K_D values. Thus, we sought to investigate whether the absolute concentration of source chemokine influenced BMDC polarization. BMDCs were exposed to a homogeneous chemokine field of CCL19 at three different concentrations (smaller than, close to, or greater than the K_D of its association with CCR7) for 10 min, after which the source concentration kept increasing at a rate such that after 30 min, the concentration in the source equaled twice that in the sink (Figure S5G).

As a result, continuously rising chemokine gradients were being established with the homogeneous pre-soak chemokine field as the background. As would be expected from receptor saturation effects, cell displacement and persistence was greatest at CCL19 concentrations close to the K_D and smallest at CCL19 concentrations much greater than the K_D, while differences in angles of trajectory and average speed were much less pronounced if the concentration was not much greater than the K_D (Figure S5H-L).

Grk3$^{-/-}$ cells show persistent migration in gradients of intermediate chemokines

To perform a stringent test of our assumption that GRK3 plays an important role for the adaptation mechanisms that temporally limit spatial sensing of intermediate chemokines we repeated the pre-soaking assays, performing a direct comparison of *Grk3*$^{-/-}$ and WT cells. As in the experiments reported in Fig. 5, we exposed cells first to a homogeneous concentration of CCL19 (for BMDC) or CXCL12 (for neutrophils) and then initiated the formation of a gradient. We found that the *Grk3*$^{-/-}$ cell populations were able to reorient in the evolving gradient that followed the initial homogeneous chemokine stimulus whereas, as reported in Fig. 5, the majority of the WT cells ignored the gradient and maintained motility along stochastically determined directions (Fig. 6). Importantly, as in Fig. 5, those WT cells that did turn into the direction of the rising gradient after the pre-soaking with the homogeneous concentration did so in an early phase of their migration, again indicating that their behavior was controlled by two phases of chemokine sensing, an initial directional orientation that was followed by temporal sensing of the absolute concentration of the stimulus.

Discussion

Here we provide data demonstrating that myeloid cells, when migrating toward intermediate chemokines (such as CCL19 and CXCL12), can detect whether the absolute concentration of a chemotactic stimulus is increasing over time and will cease to migrate persistently when it does not. In addition to their well-established spatial sensing capabilities, neutrophils and immature DC thus can read the temporal evolution of chemokine concentrations, a capacity that may be intimately linked to determining whether an infection is increasing or resolving and limiting effector cell recruitment capable of added tissue damage in the latter case. Indeed, both CCL19 and CXCL12 have been found to regulate neutrophil and dendritic cell recruitment under conditions involving responses to acute stimuli, as opposed to organismal steady states (Delano et al., 2011; Robbiani et al., 2000; Yamada et al., 2011), conditions where the cells' ability to adjust their migratory responses to the temporal evolution of the chemotactic signal may play a central role in preventing immunopathology.

Exposure of DC and neutrophils to gradients of intermediate chemokines resulted in cellular polarization based on short-term spatial sensing followed by a short-lived phase of cell migration in the direction of this initial polarization. Then, as GRK-mediated desensitization occurs, persistent migration no longer involved sensing the orientation of the gradient slope, but instead was based on cell movement along the existing polarization axis and a requirement for exposure to a rising concentration of attractant to overcome the loss in receptor sensitivity. Our findings also provide clear evidence that the mode of cell chemotactic control differs between intermediate chemokines and those such as C5a defined as 'end agonists'. Myeloid cell migration directed by intermediate chemokines involves initial spatial gradient sensing that determines cell orientation followed by temporal sensing that drives persistent migration, whereas end agonists can direct persistent migration as stable gradients.

The predominant 'spatial sensing' model proposes that a cell entering a gradient of chemoattractant detects the differences in extracellular attractant concentration across the

cell diameter via receptor-mediated signaling mechanisms. Based on as little as a 2–5% concentration difference across the cell diameter (Parent and Devreotes, 1999; Zigmond, 1977), the cell then polarizes and engages in directed migration along the upward slope of the gradient. It is widely believed that any concentration difference that can be detected by the chemosensing mechanisms of the cell is also sufficient to drive persistent directed migration. As noted previously, Lauffenburger et al. (Lauffenburger et al., 1987) argued that spatial and not temporal gradients were sufficient for directed chemotaxis of neutrophils. Interestingly, many of these early studies utilized neutrophils and fMLP, an end agonist whose capacity to induce persistent migration with stable gradients is consistent with our current data on C5a. Early work from Vicker et al. (Vicker, 1989; Vicker et al., 1986), while failing to substantially influence the prevailing spatial-sensing paradigm that has dominated since then, provided evidence that the nature of the response might depend on the ligand studied, results that agree with the more extensive analysis we have conducted here.

Most previous quantitative studies of chemotaxis have been conducted in 2D spatially-restrictive channels (Zigmond, 1977), either with flow-induced soluble gradients or with surface-bound gradients, or in semi-quantitative 3D chambers (Boyden, 1962). It is worth noting that many of the custom (Abhyankar et al., 2008; Amadi et al., 2010; Saadi et al., 2007) and commercially available gradient generators (EZ Taxiscan, Ibidi) (Bae et al., 2008; Kanegasaki et al., 2003) used in these experiments require cell introduction into the chamber, followed by gradient establishment. In these cases, there is a gradual increase in chemokine concentration throughout the device as the gradient develops until a steady state persistent stable gradient is established. Often, cell migration data in these devices has been acquired during the early rising phase, which as we show here corresponds to markedly different cell migration behavior as compared to what is observed in stable gradients of intermediate chemokines. A focus on cell behavior during this initial gradient development phase may also explain why Haessler et al. (Haessler et al., 2009), using a similar chamber design as employed here, did not report the shift from spatial to temporal sensing in their studies.

What is the origin of the requirement for rising stimulus levels for persistent migration to intermediate chemoattractants? Our study shows that negative feedback regulation of the chemokine sensing apparatus (desensitization involving GRK3) plays a central, though not necessarily exclusive, role in determining whether the cell processes spatial or temporal information about the chemokine concentration during long-range migration. Presumably, the extent of the desensitization process for receptors engaging intermediate chemokines only permits signaling sufficient to sustain locomotion when the absolute concentration of the attractant rises so that additional receptor engagement at the leading edge overcomes the desensitization process. Our previous *Dictyostelium* chemosensing studies revealed that exposure to cAMP diminishes responsiveness to the spatial gradient at the front of the cell (Xu et al., 2007), though apparently not to an extent that eliminates the capacity to receive a signal driving persistent migratory behavior. Here we speculate that a stronger desensitization and, potentially, adaptation process in myeloid cells that experience soluble fields of intermediate chemokines, results in a more potent negative feedback mechanism. Temporal increases in absolute chemokine concentration are required to drive receptor-dependent signaling at a sufficient rate to overcome such feedback. In contrast to soluble

ligands, matrix-bound chemokines lead to much slower cellular desensitization. Given our data, we speculate that spatial gradients of bound intermediate chemokines, such as CCL21, are sufficient to drive dendritic cell haptotaxis on 2D planar anatomy (Weber et al., 2013) because the velocity of the moving cell exposes its leading edge to a higher level of chemokine sufficient to overcome the slower loss of responsiveness. With soluble ligands, the migration rate is presumably too slow to overcome the faster rate of desensitization and a rising input of chemokine is needed to sustain motility. Interestingly, even for bound chemokines, the same research group recently found that exponentially increasing chemokine concentrations are required for persistent chemotaxis towards CCL21 (Schwarz et al., 2017). One possible explanation for the requirement for exponential gradients would be that in exponential gradients the relative concentration difference across the cell diameter (difference between front and back concentration divided by absolute concentration) stays constant whereas it decreases in linear gradients as the absolute concentration increases. The physical/chemical limits of receptor-mediated gradient sensing would thus dictate the requirement for exponential gradients. But while this mechanism may control haptotactic migration along surface bound chemokine gradients it does not appear to control the migration of myeloid cells in soluble gradients. This is evident from our findings that the cells migrate well in static linear end agonist gradients and that even static linear gradients of intermediate chemokines can induce prolonged chemotaxis in *Grk3*$^{-/-}$ cells.

In other biological systems, temporal rises in signaling cues can dictate cell behavior. Bacteria use temporal sensing to guide their migration; the small size of bacteria precludes effective spatial sensing across the cell length, and these organisms switch between tumbling and straight motion depending on the temporal features of the external chemoattractant signal (Macnab and Koshland, 1972). Mammalian spermatozoa distinguish temporal progesterone gradients from spatial gradients with distinct biological responses, either hyperactivation or reduced activation (Armon and Eisenbach, 2011). Perhaps most relevant to the present study is fly imaginal disc patterning, where a graded Dpp signal leads to proliferative growth that is homogeneous in space. Similar to this study, Wartlick and colleagues considered steepness of the spatial gradient as a plausible explanation, but they found that temporal sensing of 50% increases in local Dpp concentration and not assessment of the spatial gradient of Dpp across the developing wing dictated cell division and growth (Wartlick et al., 2011).

While it is easy to imagine how an adaptive temporal sensing mechanism would be effective in a time-limited development process, it is less clear how it would work in an ongoing inflammatory process of variable duration. A requirement for rising concentrations to yield robust directed migration with intermediate chemokines implies that in vivo mechanisms must operate to allow such sensing within reasonable bounds of chemokine production and tissue accumulation (Foxman et al., 1997). Possibilities include the operation of recurring local oscillations of chemokine gradients within tissue spaces, allowing cells to reset their sensitivity and persist in migration without a need for ever higher intermediate chemoattractant levels (Yde et al., 2011). Alternatively, there may be a role for time-changing levels of chemokine receptors (Sallusto et al., 1998; Sozzani et al., 1998) rather than chemokine in providing the necessary delta between input stimulus and desensitization effects, or feed-forward amplification mechanisms that produce continually rising attractant

concentrations (Brandes et al., 2013; Lammermann et al., 2008). Finally, even though we found temporal sensing to play an important role for bone-marrow derived DC and neutrophil chemotaxis toward intermediate chemokines the behavior of other cell types may be different, depending on their role during organism maintenance or immune responses. Such notions make it clear that new models and new data will be needed to more fully understand hematopoietic cell navigation from blood to distant locations in complex tissues, given the role of temporal chemokine sensing we document here for key innate immune cell populations.

STAR Methods

CONTACT FOR REAGENT AND RESOURCE SHARING

Further information and request for resources and reagents should be directed to Lead Contact, Martin Meier-Schellersheim (mms@niaid.nih.gov). CD11c-EYFP C57BL/6 (Taconic®) and *Grk3*$^{-/-}$ (Jackson®) are available commercially. The *Grk3*$^{-/-}$ DsRed$^{+/+}$ cross mouse line described in this study is available from our laboratory and requires a Material Transfer Agreement (MTA). The β-arrestin-2$^{-/-}$ mice were a donation from the RJ Lefkowitz lab, Duke Medical Center. The β-arrestin-1$^{-/-}$ mice were a donation from the JH Kehrl lab (NIAID, NIH).

EXPERIMENTAL MODEL AND SUBJECT DETAILS

Murine bone marrow-derived dendritic cells from several mouse strains (CD11c-EYFP C57BL/6 (Lindquist et al., 2004), *Grk3*$^{-/-}$, *Grk6*$^{-/-}$ (Gainetdinov et al., 2003), β-arrestin-2$^{-/-}$ (Bohn et al., 1999), β-arrestin-1$^{-/-}$ (Conner et al., 1997) and *Grk3*$^{-/-}$ C57BL/6 mice, crossed with DsRed mice to generate DsRed/*Grk3*$^{-/-}$ mice.

METHOD DETAILS

Mice, Cell Culture—Primary cells isolated from CD11c-EYFP C57BL/6 (Lindquist et al., 2004) or WT C57BL/6 mice were utilized for the majority of migration experiments. Cells isolated from *Grk3*$^{-/-}$, *Grk6*$^{-/-}$ mice (Jackson Laboratories (Line 012431 (Peppel et al., 1997) and 010961 (Gainetdinov et al., 2003), respectively), β-arrestin-2$^{-/-}$ mice (Bohn et al., 1999) (a generous donation from the RJ Lefkowitz lab, Duke Medical Center), and β-arrestin-1$^{-/-}$ mice (Conner et al., 1997) (a generous donation from the JH Kehrl lab, NIAID, NIH) were also used in the indicated experiments. *Grk3*$^{-/-}$ C57BL/6 mice were crossed with DsRed mice to generate DsRed/*Grk3*$^{-/-}$ mice to be used with CD11c-EYFP C57Bl/6 mice in co-migration experiments. All donor mice were maintained in specific-pathogen-free conditions at an Association for Assessment and Accreditation of Laboratory Animal Care-accredited animal facility at the NIAID. All procedures were approved by the NIAID Animal Care and Use Committee (National Institutes of Health, Bethesda, MD).

Murine bone marrow-derived dendritic cells were isolated as described elsewhere (Lammermann et al., 2008). Briefly, cells were flushed from mouse femurs and tibias, plated in petri dishes at 2.5 million cells per dish, and supplemented with 20ng/ml GM-CSF (Peprotech, #315-03) in base medium (10% Hyclone FBS, 1% penicillin-streptomycin in RPMI) for 7 days. Dendritic cells were then transferred to tissue culture plates and matured

overnight in 0.2ug/ml lipopolysaccharide (LPS). The non-adherent fraction of matured dendritic cells was harvested for cell migration studies. Murine neutrophils were freshly isolated from bone marrow utilizing a Percoll gradient separation method described elsewhere (Peters et al., 2008). Briefly, cells were flushed from mouse femurs and tibias, incubated with ACK buffer for 1min, under-laid in a discontinuous Percoll gradient, and spun at 1500g for 40 minutes at room temperature. Cells were harvested from the 69%/78% interface, washed 2× in buffer, and used for cell migration studies following a 30 minute incubation at 37°C.

Mask and Template Fabrication—Devices were fabricated using commercial film masks generated by high-resolution laser photoplotting (CAD/Art Services, Bandon OR). The 3-inch silicon wafers were first cleaned with solvent (acetone, methanol, and 18MΩ water and then dehydrated for 10 minutes on a 200°C hotplate. The wafers were then immediately laminated with two layers of 100μm thick DuPont WBR2000 Series dry film photoresist (Microchem, Newton MA) at a temperature of 95°C and a speed of 1mm/sec, using a hot roll laminator (model HRL 4200, Think and Tinker, Palmer Lake CO). After lamination, the wafers were baked at 65°C for 20 minutes to promote adhesion of the resist. The silicon wafers were then held in contact with the channel-patterned film mask, using a glass wafer and exposed using a collimated near-UV light source (model LS30/10, OAI, San Jose CA). An hour after exposure, the wafers were developed in a 0.85% solution of a potassium carbonate developer (RBP DX-40, Microchem, Newton MA) at 30°C for 3 minutes using a spray developer (Rotaspray, Mega-UK, Cambridge UK). Following development, the completed templates were immediately rinsed in tap water, then DI water, and finally, baked at 200°C for 10 minutes to promote resist adhesion.

Agarose Device Fabrication and Assembly—The agarose device was fabricated using the methods established by Haessler et al. (Haessler et al., 2009). First, a PDMS frame (with a thickness of 500μm) with outer dimensions of 2.5mm × 3.5mm and inner opening of 1.25mm × 2mm was cut and placed on the silicon template. After pouring melted 3% w/v agarose (SeaKem LE Agarose, Lonza, Rockland, ME) into the PDMS frame (on top of the patterned template), a glass slide was immediately placed on top, leveling the agarose at the top of the PDMS frame, and uniform pressure applied until the agarose gelled. Afterwards, the glass slide was removed and the entire agarose template was submerged in culture media.

The PDMS frame was removed from the template, rinsed with water, and allowed to dry before being placed on a #1.5 cover slide. The agarose device was then seated channel-side down in the PDMS frame, and through-holes were punched at the ends of the channels to provide inlets and outlets. A custom Plexiglas manifold with stainless steel tubes was used to provide an interface between the agarose device and the flexible tubing connected to the syringe pump. The flat lower surface of the manifold also provided mechanical support for the agarose device when the entire assembly was secured together with a metal clamping plate. The sink channel was connected to a single syringe pump containing base medium. The source channel was connected to a mixing tee supplied by two programmable pumps, with one syringe containing chemokine and the second containing base media alone. The

pump program determines the percent contribution of each stream, so that either static or dynamic chemokine concentrations could be pumped downstream of the mixing tee. Flow rates of 5μl/min per channel were maintained in parallel in just the source and sink channels. No bulk flow occurred in the collagen plus cell-containing central channel used for migration analysis.

Spatio-Temporal Chemokine Profiles—Spatio-temporal chemokine profiles were characterized using both 10kDa FITC-dextran and custom labeled Alexa-Fluor 594-CCL19 (Molecular Probes, Grand Island, NY) at 1μM in the source channel. Polymerized collagen at 1.7mg/ml final concentration was added to the center channel for all gradient characterization studies. In some studies using Alexa-Fluor 594-CCL19, dendritic cells were added along with collagen to the center channel to characterize cell influence on bulk gradient distribution. x–y images spanning the source to sink channel were collected on a Zeiss 510 inverted microscope using confocal settings and a 0.9NA 25× oil immersion objective. The pinhole diameter was set to 10μm, and separate z slices were imaged at the bottom, center, and top of the channels. 1024 × 1024 images were captured every 5–10 minutes for 1.5 hrs, similar to the time scale for the longest cell migration studies.

The relative concentration difference (RCD) values were calculated from the fluorescent images of gradient formation using the dextran model molecule. A confocal slice corresponding to the middle plane of the central channel was used, and the intensity was averaged along a 400μm length of the channel. The resulting intensity profile was normalized and corrected for dark counts, and then was fit using a Boltzmann function (y= B + A/(1+exp((x−x_0)/dx)). The resulting fitted curve was then used to calculate the RCD values, defined as RCD(x)=(I(x+dx) −I(x))/I(x). Although the Boltzmann form was chosen as a convenient means to get a sigmoidal curve, a cubic polynomial fit gave similar residual and RCD values.

3-D Migration Experiments—Cultured BMDCs or freshly isolated neutrophils were re-suspended (5×10^6 total cells) in 80 μL of base medium. 37 μL of type I bovine collagen (Purecol, Advanced Biomatrix, San Diego, CA) were gently mixed with 5 μL 10× DMEM and 2.5 μL sodium bicarbonate. The collagen mixture was then added to the 80 μL cell suspension. In 10 μL aliquots, the cell-collagen suspension was loaded into the center channel of the microfluidic device until filled. The device was incubated at 37°C while the collagen crosslinked, and inverted every 5 minutes to ensure uniform cell distribution in z.

Following collagen crosslinking, tubing for the input and output ports was connected to the source and sink channels, and the device was transferred to a Zeiss 510 confocal microscope stage with 37°C heating. Syringe pumps were set to 5 μl/min continuous pumping. For dendritic cell chemotaxis, final source chemokine concentrations were CXCL12 = 30nM, C5a = 10nM, and CCL19 ranged from 0.5 – 50nM. For neutrophil cell chemotaxis, final source chemokine concentrations were CXCL12 = 30nM and C5a = 5nM. For pre-set chemokine gradient runs, the device was assembled without cells and collagen infused into the center channel. Gradients were pre-established by pumping chemokine through the source channel and medium through the sink channel for 30 minutes. The cell-collagen suspension was then introduced into the center channel and pumping of the source and sink

channels resumed following collagen gelation. For pre-soaking experiments, 3% agarose devices were soaked in chemokine solution overnight. Chemokine was added to the cell-collagen suspension at a concentration similar to the pre-soaked agarose prior to the introduction of cells into the device. During the experiment, this same chemokine concentration was maintained in the sink channel, while a higher chemokine concentration was introduced in the source channel to create a spatial gradient. For dendritic cell experiments, presoaking CCL19 concentrations ranged from 0.1nM to 50nM (<<<Kd, = Kd, or >>>Kd). For neutrophil experiments, presoaking concentrations for C5a and CXCL12 were 0.05nM and 0.3nM, respectively.

EZ Taxiscan Experiments—A 2D microchemotaxis chamber (TAXIScan; Effector Cell Institute) was used to detect real-time horizontal chemotaxis. After LPS stimulation, mature DCs were seeded to one side of the chamber and 0.5nM CCL19 was added to the opposite side. Cells entered the 2D spatially-restricted microchambers (5 μm height) and migrated towards the source well along a BSA-coated glass coverslip. Stable gradients developed within 5–10 minutes according to manufacturer's specifications and cells traversed ¾ of the chamber length within 30 minutes. Microchambers were maintained at 37°C and phase images were collected every 15 seconds with a CCD camera.

QUANTIFICATION AND STATISTICAL ANALYSIS

Raw image files were taken on a Zeiss 510 inverted confocal microscope using a 0.9NA 25× oil objective. For cell migration tracking experiments, average field size was 330 μm × 330 μm with pixel resolution, 2.34 pixels = 1 μm. Gradient characterization studies involved imaging at 5–10 minute intervals, dendritic cell migration studies at 45 second intervals, and neutrophil migration studies at 20 second intervals. Raw image files were imported into Imaris imaging software (version 7.1). The Tracking Spots application was used to generate displacement, path length, speed, and velocity data points. Across cell migration experiments, a variable number of cells showed active migration in different conditions, thus, representative tracks are shown only for those that clearly polarize and migrate. The Snapshot tool was utilized to generate time-lapse movies (with 6fps playback), still images, and track histories. From these statistics, chemotactic metrics were calculated in Excel and data were plotted in Prism. Significance for each experimental comparison was determined utilizing an unpaired T-test and all error bars are reported as SEM.

Supplementary Material

Refer to Web version on PubMed Central for supplementary material.

References

Abhyankar VV, Toepke MW, Cortesio CL, Lokuta MA, Huttenlocher A, Beebe DJ. A platform for assessing chemotactic migration within a spatiotemporally defined 3D microenvironment. Lab Chip. 2008; 8:1507–1515. [PubMed: 18818806]

Amadi OC, Steinhauser ML, Nishi Y, Chung S, Kamm RD, McMahon AP, Lee RT. A low resistance microfluidic system for the creation of stable concentration gradients in a defined 3D microenvironment. Biomed Microdevices. 2010; 12:1027–1041. [PubMed: 20661647]

Armon L, Eisenbach M. Behavioral mechanism during human sperm chemotaxis: involvement of hyperactivation. PLoS One. 2011; 6:e28359. [PubMed: 22163296]

Arrieumerlou C, Meyer T. A local coupling model and compass parameter for eukaryotic chemotaxis. Dev Cell. 2005; 8:215–227. [PubMed: 15691763]

Bae SY, Jung YJ, Woo SY, Park MH, Seoh JY, Ryu KH. Distinct locomotive patterns of granulocytes, monocytes and lymphocytes in a stable concentration gradient of chemokines. Int J Lab Hematol. 2008; 30:139–148. [PubMed: 18333846]

Balabanian K, Levoye A, Klemm L, Lagane B, Hermine O, Harriague J, Baleux F, Arenzana-Seisdedos F, Bachelerie F. Leukocyte analysis from WHIM syndrome patients reveals a pivotal role for GRK3 in CXCR4 signaling. J Clin Invest. 2008; 118:1074–1084. [PubMed: 18274673]

Bohn LM, Lefkowitz RJ, Gainetdinov RR, Peppel K, Caron MG, Lin FT. Enhanced morphine analgesia in mice lacking beta-arrestin 2. Science. 1999; 286:2495–2498. [PubMed: 10617462]

Boyden S. The chemotactic effect of mixtures of antibody and antigen on polymorphonuclear leucocytes. J Exp Med. 1962; 115:453–466. [PubMed: 13872176]

Brandes M, Klauschen F, Kuchen S, Germain RN. A systems analysis identifies a feedforward inflammatory circuit leading to lethal influenza infection. Cell. 2013; 154:197–212. [PubMed: 23827683]

Byers MA, Calloway PA, Shannon L, Cunningham HD, Smith S, Li F, Fassold BC, Vines CM. Arrestin 3 mediates endocytosis of CCR7 following ligation of CCL19 but not CCL21. J Immunol. 2008; 181:4723–4732. [PubMed: 18802075]

Campbell JJ, Foxman EF, Butcher EC. Chemoattractant receptor cross talk as a regulatory mechanism in leukocyte adhesion and migration. Eur J Immunol. 1997; 27:2571–2578. [PubMed: 9368612]

Castellino F, Huang AY, Altan-Bonnet G, Stoll S, Scheinecker C, Germain RN. Chemokines enhance immunity by guiding naive CD8+ T cells to sites of CD4+ T cell-dendritic cell interaction. Nature. 2006; 440:890–895. [PubMed: 16612374]

Charest PG, Firtel RA. Feedback signaling controls leading-edge formation during chemotaxis. Curr Opin Genet Dev. 2006; 16:339–347. [PubMed: 16806895]

Chenoweth DE, Goodman MG. The C5a receptor of neutrophils and macrophages. Agents Actions Suppl. 1983; 12:252–273. [PubMed: 6573117]

Comerford I, Milasta S, Morrow V, Milligan G, Nibbs R. The chemokine receptor CCX-CKR mediates effective scavenging of CCL19 in vitro. Eur J Immunol. 2006; 36:1904–1916. [PubMed: 16791897]

Conner DA, Mathier MA, Mortensen RM, Christe M, Vatner SF, Seidman CE, Seidman JG. beta-Arrestin1 knockout mice appear normal but demonstrate altered cardiac responses to beta-adrenergic stimulation. Circ Res. 1997; 81:1021–1026. [PubMed: 9400383]

Delano MJ, Kelly-Scumpia KM, Thayer TC, Winfield RD, Scumpia PO, Cuenca AG, Harrington PB, O'Malley KA, Warner E, Gabrilovich S, et al. Neutrophil mobilization from the bone marrow during polymicrobial sepsis is dependent on CXCL12 signaling. J Immunol. 2011; 187:911–918. [PubMed: 21690321]

Ebrahimzadeh PR, Hogfors C, Braide M. Neutrophil chemotaxis in moving gradients of fMLP. J Leukoc Biol. 2000; 67:651–661. [PubMed: 10811005]

Foxman EF, Campbell JJ, Butcher EC. Multistep navigation and the combinatorial control of leukocyte chemotaxis. J Cell Biol. 1997; 139:1349–1360. [PubMed: 9382879]

Gainetdinov RR, Bohn LM, Sotnikova TD, Cyr M, Laakso A, Macrae AD, Torres GE, Kim KM, Lefkowitz RJ, Caron MG, et al. Dopaminergic supersensitivity in G protein-coupled receptor kinase 6-deficient mice. Neuron. 2003; 38:291–303. [PubMed: 12718862]

Haessler U, Kalinin Y, Swartz MA, Wu M. An agarose-based microfluidic platform with a gradient buffer for 3D chemotaxis studies. Biomed Microdevices. 2009; 11:827–835. [PubMed: 19343497]

Kanegasaki S, Nomura Y, Nitta N, Akiyama S, Tamatani T, Goshoh Y, Yoshida T, Sato T, Kikuchi Y. A novel optical assay system for the quantitative measurement of chemotaxis. J Immunol Methods. 2003; 282:1–11. [PubMed: 14604536]

Kavelaars A, Vroon A, Raatgever RP, Fong AM, Premont RT, Patel DD, Lefkowitz RJ, Heijnen CJ. Increased acute inflammation, leukotriene B4-induced chemotaxis, and signaling in mice deficient for G protein-coupled receptor kinase 6. J Immunol. 2003; 171:6128–6134. [PubMed: 14634128]

Kohout TA, Nicholas SL, Perry SJ, Reinhart G, Junger S, Struthers RS. Differential desensitization, receptor phosphorylation, beta-arrestin recruitment, and ERK1/2 activation by the two endogenous ligands for the CC chemokine receptor 7. J Biol Chem. 2004; 279:23214–23222. [PubMed: 15054093]

Lammermann T, Bader BL, Monkley SJ, Worbs T, Wedlich-Soldner R, Hirsch K, Keller M, Forster R, Critchley DR, Fassler R, et al. Rapid leukocyte migration by integrin-independent flowing and squeezing. Nature. 2008; 453:51–55. [PubMed: 18451854]

Lauffenburger D, Farrell B, Tranquillo R, Kistler A, Zigmond S. Gradient perception by neutrophil leucocytes, continued. J Cell Sci. 1987; 88(Pt 4):415–416. [PubMed: 3503899]

Lauffenburger DA, Tranquillo RT, Zigmond SH. Concentration gradients of chemotactic factors in chemotaxis assays. Methods Enzymol. 1988; 162:85–101. [PubMed: 3226329]

Levine H, Kessler DA, Rappel WJ. Directional sensing in eukaryotic chemotaxis: a balanced inactivation model. Proc Natl Acad Sci U S A. 2006; 103:9761–9766. [PubMed: 16782813]

Lin F, Butcher EC. Modeling the role of homologous receptor desensitization in cell gradient sensing. J Immunol. 2008; 181:8335–8343. [PubMed: 19050250]

Lindquist RL, Shakhar G, Dudziak D, Wardemann H, Eisenreich T, Dustin ML, Nussenzweig MC. Visualizing dendritic cell networks in vivo. Nat Immunol. 2004; 5:1243–1250. [PubMed: 15543150]

Link A, Vogt TK, Favre S, Britschgi MR, Acha-Orbea H, Hinz B, Cyster JG, Luther SA. Fibroblastic reticular cells in lymph nodes regulate the homeostasis of naive T cells. Nat Immunol. 2007; 8:1255–1265. [PubMed: 17893676]

Ma L, Janetopoulos C, Yang L, Devreotes PN, Iglesias PA. Two complementary, local excitation, global inhibition mechanisms acting in parallel can explain the chemoattractant-induced regulation of PI(3,4,5)P3 response in dictyostelium cells. Biophys J. 2004; 87:3764–3774. [PubMed: 15465874]

Macnab RM, Koshland DE Jr. The gradient-sensing mechanism in bacterial chemotaxis. Proc Natl Acad Sci U S A. 1972; 69:2509–2512. [PubMed: 4560688]

Meier-Schellersheim M, Xu X, Angermann B, Kunkel EJ, Jin T, Germain RN. Key role of local regulation in chemosensing revealed by a new molecular interaction-based modeling method. PLoS Comput Biol. 2006; 2:e82. [PubMed: 16854213]

Meinhardt H. Orientation of chemotactic cells and growth cones: models and mechanisms. J Cell Sci. 1999; 112(Pt 17):2867–2874. [PubMed: 10444381]

Milcent MD, Christophe T, Rabiet MJ, Tardif M, Boulay F. Overexpression of wild-type and catalytically inactive forms of GRK2 and GRK6 fails to alter the agonist-induced phosphorylation of the C5a receptor (CD88): evidence that GRK6 is autophosphorylated in COS-7 cells. Biochem Biophys Res Commun. 1999; 259:224–229. [PubMed: 10334944]

Nagira M, Imai T, Hieshima K, Kusuda J, Ridanpaa M, Takagi S, Nishimura M, Kakizaki M, Nomiyama H, Yoshie O. Molecular cloning of a novel human CC chemokine secondary lymphoid-tissue chemokine that is a potent chemoattractant for lymphocytes and mapped to chromosome 9p13. J Biol Chem. 1997; 272:19518–19524. [PubMed: 9235955]

Parent CA, Devreotes PN. A cell's sense of direction. Science. 1999; 284:765–770. [PubMed: 10221901]

Peppel K, Boekhoff I, McDonald P, Breer H, Caron MG, Lefkowitz RJ. G protein-coupled receptor kinase 3 (GRK3) gene disruption leads to loss of odorant receptor desensitization. J Biol Chem. 1997; 272:25425–25428. [PubMed: 9325250]

Peters NC, Egen JG, Secundino N, Debrabant A, Kimblin N, Kamhawi S, Lawyer P, Fay MP, Germain RN, Sacks D. In vivo imaging reveals an essential role for neutrophils in leishmaniasis transmitted by sand flies. Science. 2008; 321:970–974. [PubMed: 18703742]

Postma M, Van Haastert PJ. A diffusion-translocation model for gradient sensing by chemotactic cells. Biophys J. 2001; 81:1314–1323. [PubMed: 11509347]

Ren XR, Reiter E, Ahn S, Kim J, Chen W, Lefkowitz RJ. Different G protein-coupled receptor kinases govern G protein and beta-arrestin-mediated signaling of V2 vasopressin receptor. Proc Natl Acad Sci U S A. 2005; 102:1448–1453. [PubMed: 15671180]

Robbiani DF, Finch RA, Jager D, Muller WA, Sartorelli AC, Randolph GJ. The leukotriene C(4) transporter MRP1 regulates CCL19 (MIP-3beta, ELC)-dependent mobilization of dendritic cells to lymph nodes. Cell. 2000; 103:757–768. [PubMed: 11114332]

Rot A, von Andrian UH. Chemokines in innate and adaptive host defense: basic chemokinese grammar for immune cells. Annu Rev Immunol. 2004; 22:891–928. [PubMed: 15032599]

Saadi W, Rhee SW, Lin F, Vahidi B, Chung BG, Jeon NL. Generation of stable concentration gradients in 2D and 3D environments using a microfluidic ladder chamber. Biomed Microdevices. 2007; 9:627–635. [PubMed: 17530414]

Sallusto F, Schaerli P, Loetscher P, Schaniel C, Lenig D, Mackay CR, Qin S, Lanzavecchia A. Rapid and coordinated switch in chemokine receptor expression during dendritic cell maturation. Eur J Immunol. 1998; 28:2760–2769. [PubMed: 9754563]

Sarris M, Masson JB, Maurin D, Van der Aa LM, Boudinot P, Lortat-Jacob H, Herbomel P. Inflammatory chemokines direct and restrict leukocyte migration within live tissues as glycan-bound gradients. Curr Biol. 2012; 22:2375–2382. [PubMed: 23219724]

Schwarz J, Bierbaum V, Vaahtomeri K, Hauschild R, Brown M, de Vries I, Leithner A, Reversat A, Merrin J, Tarrant T, et al. Dendritic Cells Interpret Haptotactic Chemokine Gradients in a Manner Governed by Signal-to-Noise Ratio and Dependent on GRK6. Curr Biol. 2017; 27:1314–1325. [PubMed: 28457871]

Sozzani S, Allavena P, D'Amico G, Luini W, Bianchi G, Kataura M, Imai T, Yoshie O, Bonecchi R, Mantovani A. Differential regulation of chemokine receptors during dendritic cell maturation: a model for their trafficking properties. J Immunol. 1998; 161:1083–1086. [PubMed: 9686565]

Tanabe S, Lu Z, Luo Y, Quackenbush EJ, Berman MA, Collins-Racie LA, Mi S, Reilly C, Lo D, Jacobs KA, et al. Identification of a new mouse beta-chemokine, thymus-derived chemotactic agent 4, with activity on T lymphocytes and mesangial cells. J Immunol. 1997; 159:5671–5679. [PubMed: 9548511]

van de Pavert SA, Mebius RE. New insights into the development of lymphoid tissues. Nat Rev Immunol. 2010; 10:664–674. [PubMed: 20706277]

Vicker MG. Gradient and temporal signal perception in chemotaxis. J Cell Sci. 1989; 92(Pt 1):1–4. [PubMed: 2674162]

Vicker MG, Lackie JM, Schill W. Neutrophil leucocyte chemotaxis is not induced by a spatial gradient of chemoattractant. J Cell Sci. 1986; 84:263–280. [PubMed: 3805156]

Wartlick O, Mumcu P, Kicheva A, Bittig T, Seum C, Julicher F, Gonzalez-Gaitan M. Dynamics of Dpp signaling and proliferation control. Science. 2011; 331:1154–1159. [PubMed: 21385708]

Weber M, Hauschild R, Schwarz J, Moussion C, de Vries I, Legler DF, Luther SA, Bollenbach T, Sixt M. Interstitial dendritic cell guidance by haptotactic chemokine gradients. Science. 2013; 339:328–332. [PubMed: 23329049]

Wisler JW, Xiao K, Thomsen AR, Lefkowitz RJ. Recent developments in biased agonism. Curr Opin Cell Biol. 2014; 27:18–24. [PubMed: 24680426]

Wu D, Lin F. Modeling cell gradient sensing and migration in competing chemoattractant fields. PLoS One. 2011; 6:e18805. [PubMed: 21559528]

Xu X, Meier-Schellersheim M, Yan J, Jin T. Locally controlled inhibitory mechanisms are involved in eukaryotic GPCR-mediated chemosensing. J Cell Biol. 2007; 178:141–153. [PubMed: 17606871]

Yamada M, Kubo H, Kobayashi S, Ishizawa K, He M, Suzuki T, Fujino N, Kunishima H, Hatta M, Nishimaki K, et al. The increase in surface CXCR4 expression on lung extravascular neutrophils and its effects on neutrophils during endotoxin-induced lung injury. Cell Mol Immunol. 2011; 8:305–314. [PubMed: 21460863]

Yde P, Mengel B, Jensen MH, Krishna S, Trusina A. Modeling the NF-kappaB mediated inflammatory response predicts cytokine waves in tissue. BMC Syst Biol. 2011; 5:115. [PubMed: 21771307]

Yoshida R, Nagira M, Kitaura M, Imagawa N, Imai T, Yoshie O. Secondary lymphoid-tissue chemokine is a functional ligand for the CC chemokine receptor CCR7. J Biol Chem. 1998; 273:7118–7122. [PubMed: 9507024]

Zidar DA, Violin JD, Whalen EJ, Lefkowitz RJ. Selective engagement of G protein coupled receptor kinases (GRKs) encodes distinct functions of biased ligands. Proc Natl Acad Sci U S A. 2009; 106:9649–9654. [PubMed: 19497875]

Zigmond SH. Ability of polymorphonuclear leukocytes to orient in gradients of chemotactic factors. J Cell Biol. 1977; 75:606–616. [PubMed: 264125]

Highlights

- Spatial cues initiate cell polarization in gradients of intermediate chemokines.
- Persistent migration to intermediate chemokines involves temporal sensing.
- G-coupled receptor kinase-dependent negative feedback prevents prolonged migration.
- Spatial cues are sufficient for persistent migration to end agonist attractants.

Eukaryotic cells are known to perform directional migration along gradients of chemoattractants. Dr. Aronin discovered that, for myeloid cells, certain (intermediate) chemokines need to have increasing absolute concentration over time to induce persistent migration, indicating that these cells are capable of sensing the temporal evolution of an immunological recruitment signal.

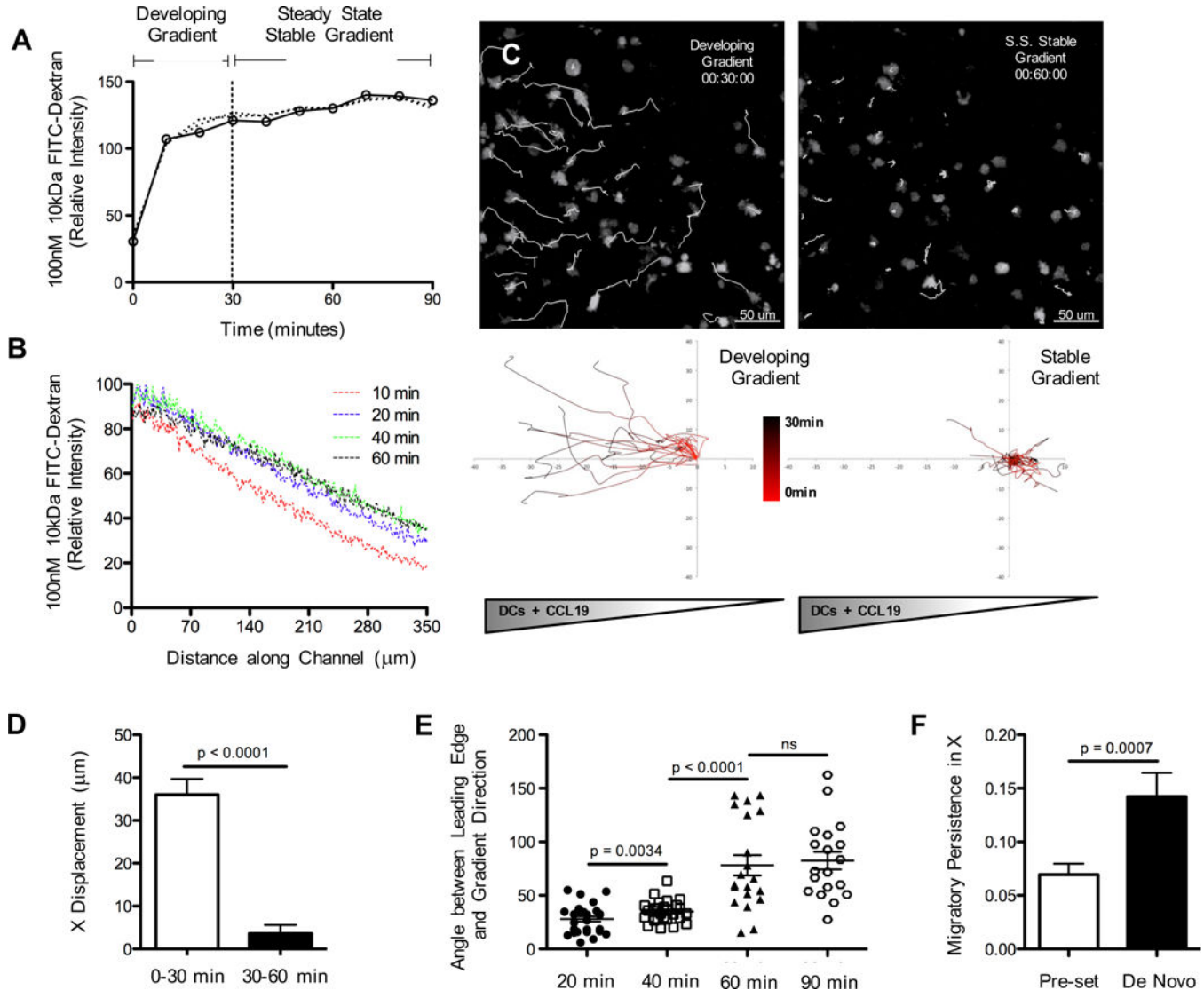

Figure 1. Distinct chemotactic responses of dendritic cells in developing vs. stable soluble gradients

(A) De novo gradient development analyzed with a model soluble molecule, 10kDa FITC-dextran. Measurements taken at the center point of a collagen-filled chamber across time as FITC-dextran diffuses from a constant source. **(B)** Temporal evolution of FITC-dextran concentration (gradient levels) across channel width (1–350μm) at z = 100 μm. **(C)** Migratory behavior of LPS-matured CD11c-EYFP BMDC (migratory tracks in white) in response to de novo gradient formation with a prolonged early rising phase (00:30:00 hrs:min:sec) and late stage steady-state (00:60:00) soluble spatial gradient of CCL19. **(D)** Total displacements of BMDC along the gradient (x)-axis at early and late stages of de novo gradient formation. Each bar is representative of 4 experiments with ~10–20 cell tracks per group, mean ± s.e.m. **(E)** Angle between the cell's leading edge and the gradient axis (0° = travelling toward, 90° = travelling perpendicular, 180° = travelling away) during early and late stage gradient formation. Representative data pooled from 2 experiments with ~8–10 measurements per group, mean ± s.e.m. **(F)** Migratory persistence along x-axis for BMDC

exposed to either a ‘de novo’ stable gradient or a ‘pre-set’ gradient (established within the agarose prior to the introduction of cells) for 60 minutes. Stable gradients in all future figures refer to ‘pre-set’ formation, rather than ‘de novo.’ Each bar is representative of 4 experiments with ~10–20 cell tracks per group, mean ± s.e.m. See also Figures S2, S3 and Movies S2, S3.

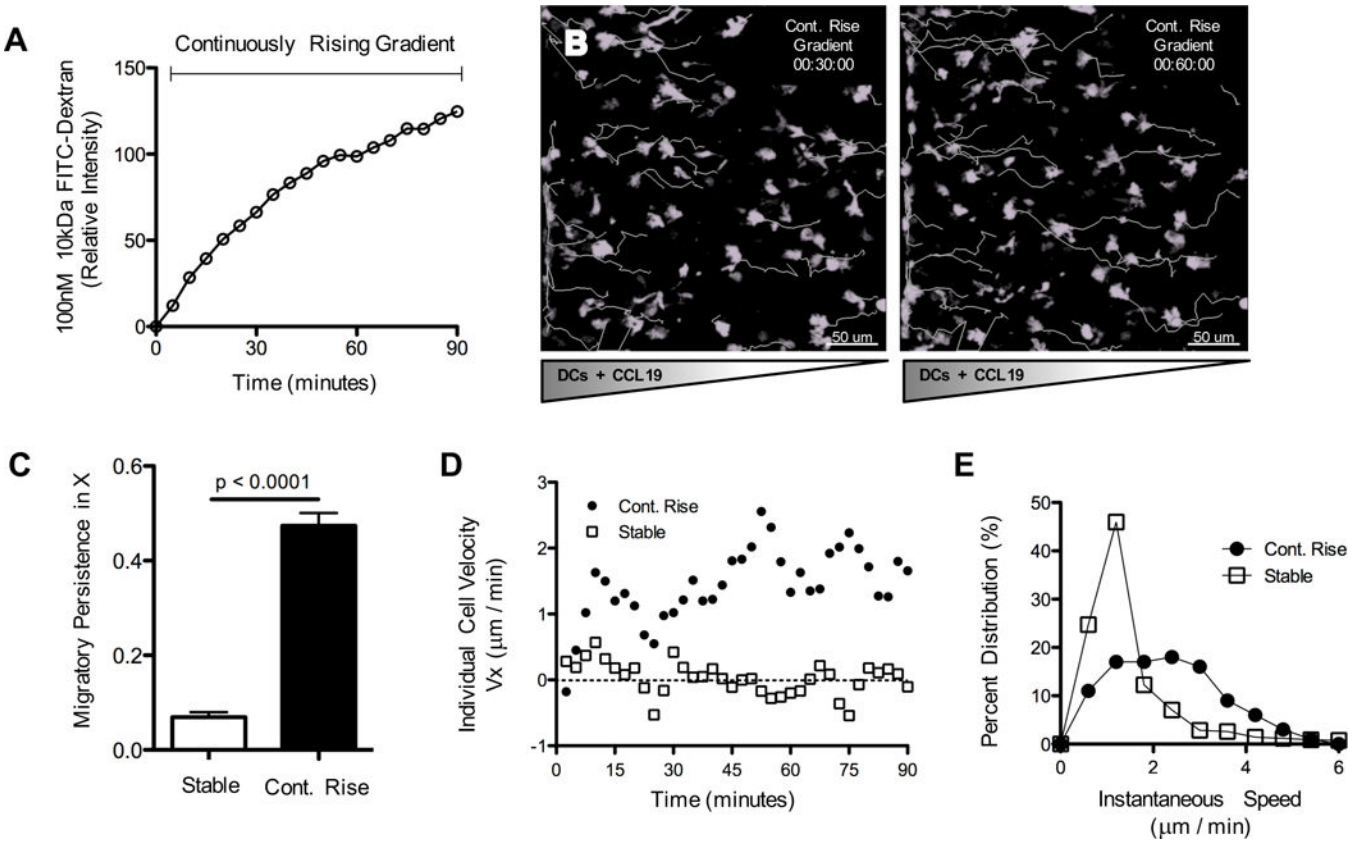

Figure 2. Temporally rising CCL19 concentration is required for persistent BMDC chemotaxis

(A) Gradient analysis using 10kDa FITC-dextran. Measurements taken at the center point within a collagen-filled chamber across time as FITC-dextran diffuses from a source with continuously rising concentration. **(B)** Migratory behavior of LPS-matured CD11c-EYFP BMDC (migratory tracks in white) in response to a continuously rising source of CCL19. **(C)** Migratory persistence along the x-axis of BMDC exposed to either stable or continuously rising source concentrations for 60 minutes. Each bar is representative of 4 experiments with ~10–20 cell tracks per group, mean ± s.e.m. **(D)** Representative individual cell velocities (+ indicates towards source, - indicates away from source) plotted across time. **(E)** Histogram of instantaneous speeds across all cell tracks and all time points. Data pooled from 4 experiments with ~10–20 cell tracks per group. See also Figures S2, S3 and Movie S5.

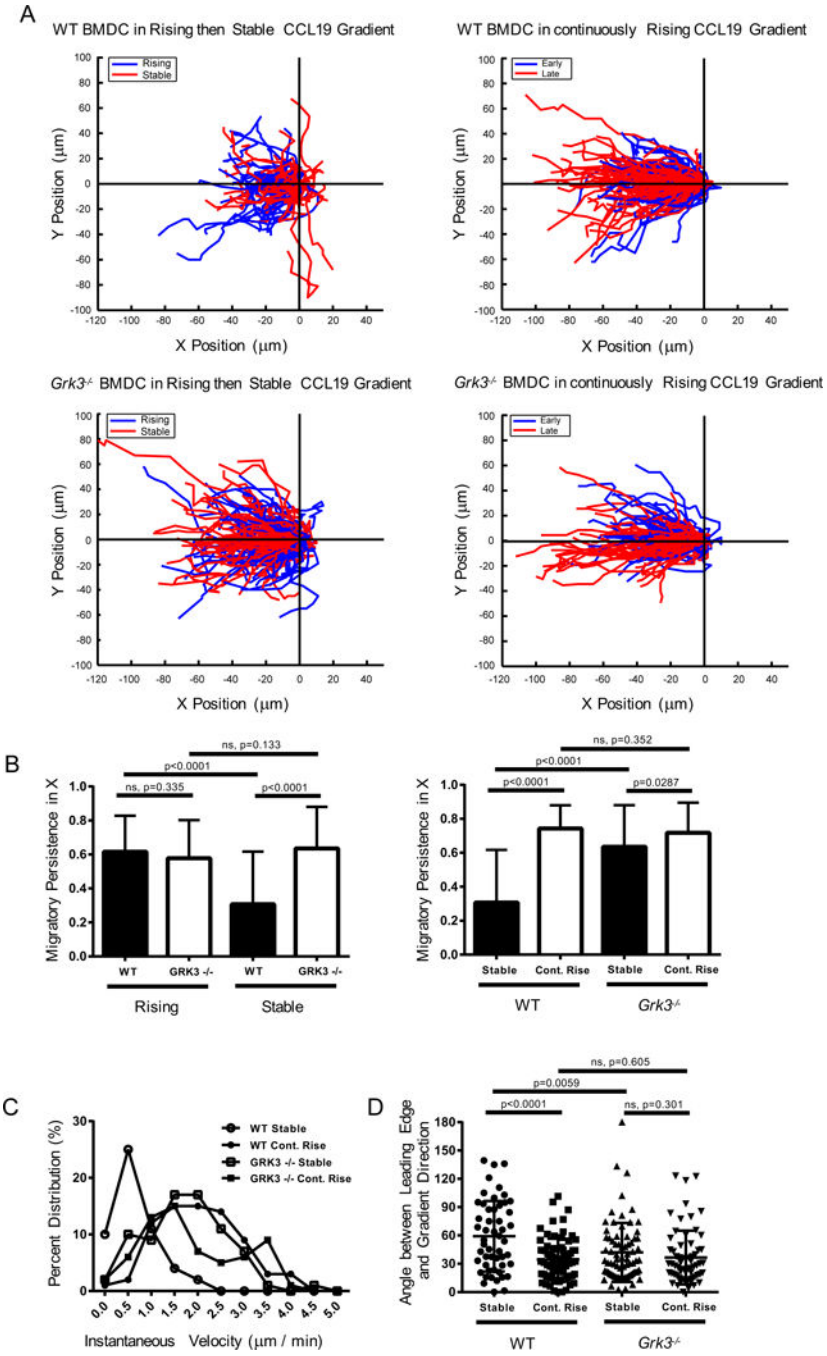

Figure 3. GRK-mediated receptor desensitization determines differential BMDC chemotactic behavior to rising then stable or continuously rising CCL19 concentrations

LPS-matured CD11c-EYFP (WT) and *DsRed/Grk3*$^{-/-}$ (GRK3) BMDC were mixed at a 1:1 ratio and added to the migration chamber. Each imaging experiment was recorded for 90 minutes, with the first and last 30 minutes labeled as “Early” and “Late” periods. For rising and stable gradient setups, the “Early” and “Late” periods corresponded to “Rising” and “Stable” phases, respectively. Tracking results derive only from experiments in which co-migration of both WT and *Grk3*$^{-/-}$ BMDCs were recorded in response to “rising and stable”

or “continuously rising” CCL19 gradients. **(A)** Overlay of individual cell tracks of co-migrating WT and GRK3 BMDC during “Rising” (Blue) or “Stable” (Red) phases in response to rising then stable gradient, or during “Early” (Blue) and “Late” (Red) phases in response to continuously rising gradient. Tracks represent aggregate data from 4 co-migration experiments each consisting of rising then stable or continuously rising gradient exposure. **(B)** Migratory persistence along the x-axis of BMDC in co-migration experiments during “Rising” and “Stable” phases of the rising then stable gradient set-up are directly compared, followed by comparison of the “Stable” phases of the rising then stable gradient set-up with the “Late” period of the continuously rising gradient set-up. Each bar is representative of at least 4 experiments with ~10–20 cell tracks per group, mean ± s.e.m. **(C)** Histogram of instantaneous speeds across all cell tracks and all time points in co-migration experiments of rising then stable gradient set-up. Data pooled from 4 experiments with 10-20 cell tracks per group. **(D)** Angle between the cell’s leading edge and the gradient axis measured during stable and rising phases following gradient input (0° = travelling toward, 90° = travelling perpendicular, 180° = travelling away). Representative data pooled from 4 experiments with ~10–20 measurements per group, mean ± s.e.m. See also Figure S4, Movie S6, and Movie S7.

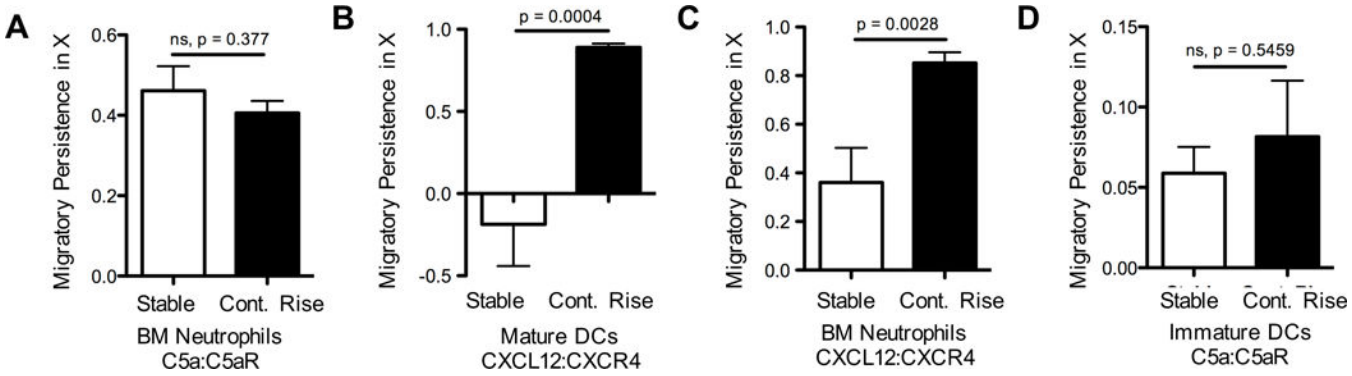

Figure 4. Temporal sensing requirement is chemokine-specific

Migratory persistence of **(A, C)** freshly isolated neutrophils**, (B)** LPS-matured BMDC (cultured 9 days), and **(D)** immature dendritic cells (cultured 6 days) in response to stable or continuously rising source concentrations. Migratory persistence along the gradient (x)-axis a shows differential chemotactic behavior based on chemokine type: C5a, **(A, D)** or CXCL12, **(B, C)**. Data pooled from 2 experiments with ~10–20 cell tracks per group, mean ± s.e.m. See also Figure S4 and Movies S8, S9.

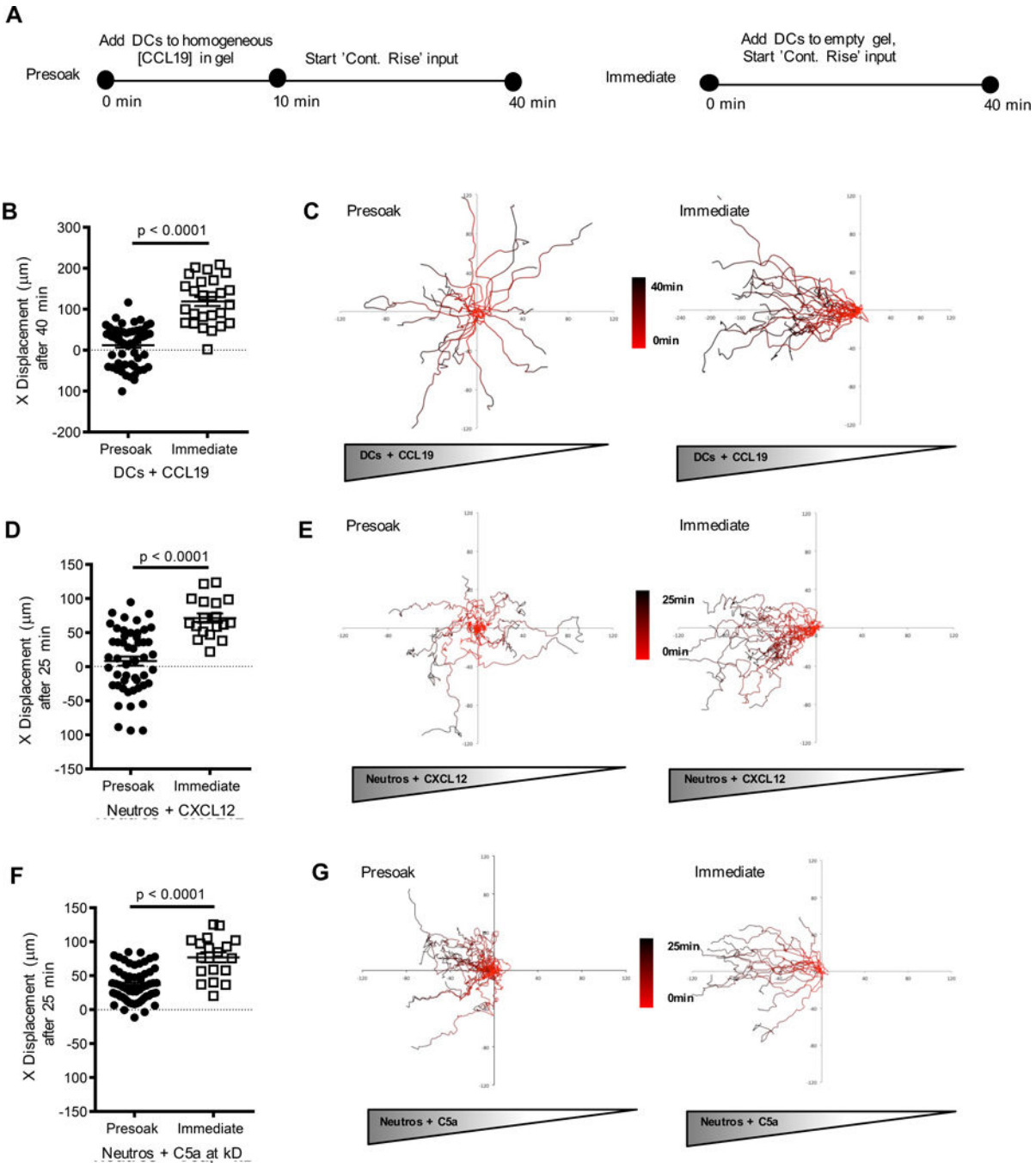

Figure 5. Following initial polarization, myeloid cells re-orient along spatial gradients of end agonist but not intermediate chemokines

(A) Cells were exposed to a spatially homogeneous chemokine concentration for 10 minutes (Figure S5) followed by a gradient with a continuously rising source (‘Presoak’) that, within 30 minutes, reached twice the initial concentration of 0.3 nM and compared with cells exposed only to a gradient with a continuously rising source (without presoaking) (‘Immediate’). **(B, D, F)** x-displacement in a chemokine gradient of cells exposed to either ‘Presoak’ or ‘Immediate’ conditions. Color scale bars (red to black, corresponding to 0 min

to 40 min) were used to indicate cell positions at specific times in the track. Data representative of 2 experiments with ~10–20 cell tracks per group, mean + s.e.m. (**C**, **E**, **G**) Individual cell tracks plotted from a common starting coordinate. See also Figure S5 and Movies S10, S11.

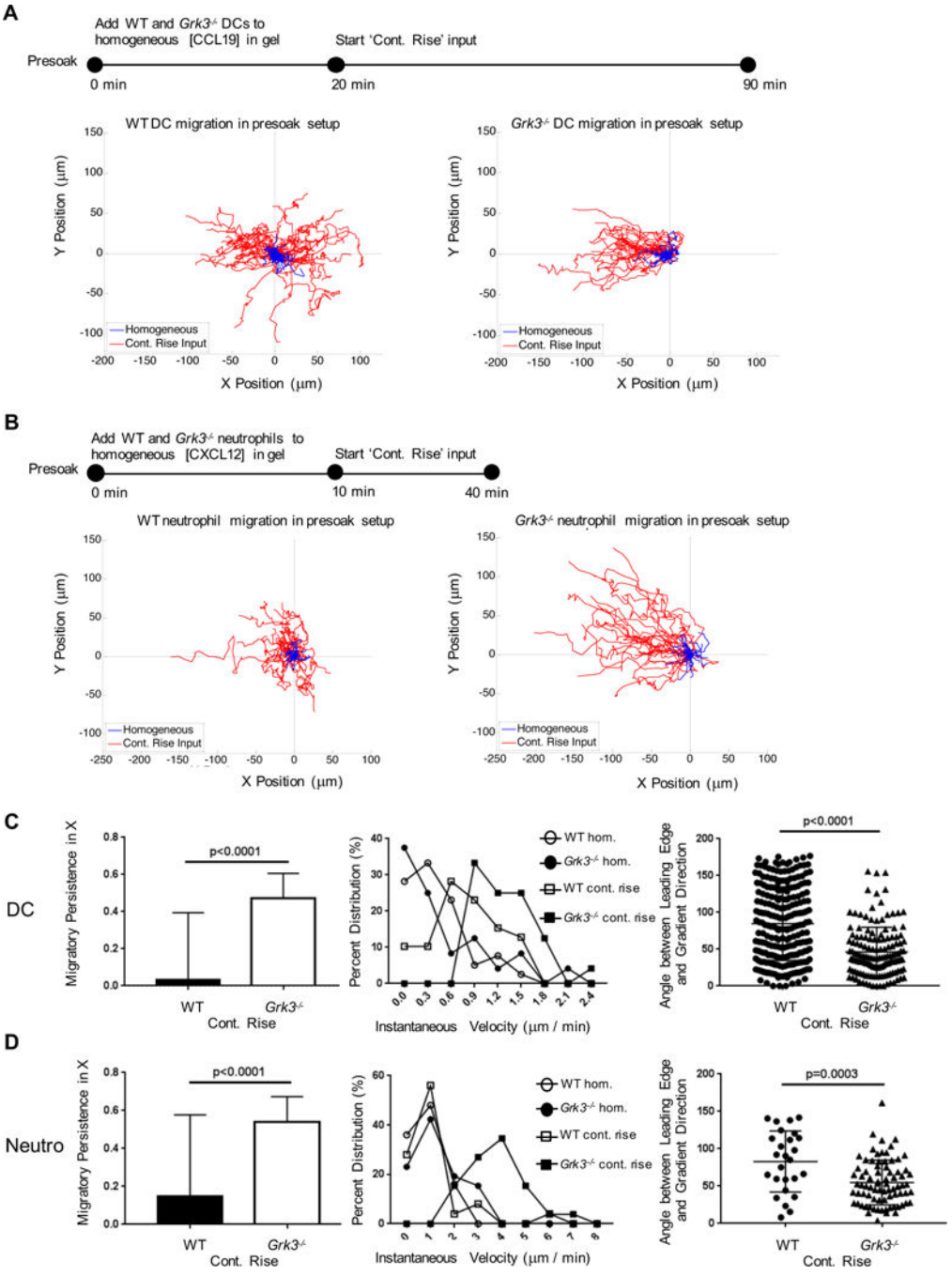

Figure 6. Prolonged chemotaxis of GRK3-deficient cells along gradients of intermediate chemokines

(A) As in the experiments described in Fig. 5, WT BMDC were exposed to a spatially homogeneous CCL19 chemokine concentration for 20 minutes followed by a gradient with a continuously rising source and compared with GRK3-deficient BMDCs exposed to the same stimuli within the same assay (simultaneously). **(B)** As in the experiments described in Fig. 5, WT neutrophils were exposed to a spatially homogeneous CXCL12 chemokine concentration for 10 minutes followed by a gradient with a continuously rising source and

compared with GRK3-deficient BMDCs exposed to the same stimuli within the same assay (simultaneously). (C, D) Migratory persistence, instantaneous velocity and the angle between the cells' leading edges and the gradient direction were quantified for BMDC (C) and neutrophils (D). See also Movies S12, S13.

Table 1

Summary of cell migratory responses divided by chemokine type (intermediate vs. end agonist), cell type (BMDCs and neutrophils, WT and GRK3-deficient), chemoattractant (CCL19, CXCL12, C5a), and source input (stable v. continuous rise, homogeneous, presoak v. immediate).

Chemokine	Cell Type	Migratory Persistence Up Spatial Gradient		Directional Path of Early Migration	Directional Path of Persistent Migration	
		Stable	Cont. Rise	Homogenous	Presoak	Immediate
CCL19	Mature DCs WT	None (Fig 1)	Directed (Fig 2)	Random (S. Fig 12)	Random (Fig 5)	Up Spatial Gradient (Fig 5)
CCL19	Mature DCs *Grk3*$^{-/-}$	Directed (Fig 3)	Directed (Fig 3)	Random (Fig 6)	Up Spatial Gradient (Fig 6)	–
CXCL12	Mature DCs WT	None (Fig 4)	Directed (Fig 4)	–	–	–
CXCL12	Neutrophils WT	None (Fig 4)	Directed (Fig 4)	Random (S. Fig 12)	Random (Fig 5)	Up Spatial Gradient (Fig 5)
CXCL12	Neutrophils *Grk3*$^{-/-}$	–	–	Random (Fig 6)	Up Spatial Gradient (Fig 6)	–
C5a	Immature DCs WT	Directed (Fig 4)	Directed (Fig 4)	–	–	–
C5a	Neutrophils WT	Directed (Fig 4)	Directed (Fig 4)	Random (S. Fig 12)	Up Spatial Gradient (Fig 5)	Up Spatial Gradient (Fig 5)